1-2021

Influence of Mechanical Layering and Natural Fractures on Undercutting and Rapid Headward Erosion (Recession) at Canyon Lake Spillway, Texas, U.S.A

Nathaniel S. Ledbetter Ferrill
Trinity University, nathanielferrill@gmail.com

David A. Ferrill

Repository Citation

Ledbetter Ferrill, N. S., & Ferrill, D. A. (2021). Influence of mechanical layering and natural fractures on undercutting and rapid headward erosion (recession) at Canyon Lake spillway, Texas, U.S.A. *Engineering Geology, 280*, Article 105897. https://doi.org/10.1016/j.enggeo.2020.105897

Engineering Geology 280 (2021) 105897

Contents lists available at ScienceDirect

Engineering Geology

journal homepage: www.elsevier.com/locate/enggeo

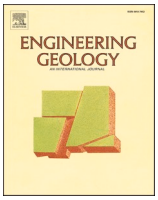

Influence of mechanical layering and natural fractures on undercutting and rapid headward erosion (recession) at Canyon Lake spillway, Texas, U.S.A

Nathaniel S. Ledbetter Ferrill [a], David A. Ferrill [b,*]

[a] Geosciences Department, Trinity University, San Antonio, TX, USA
[b] Space Science and Engineering Division, Southwest Research Institute, San Antonio, TX, USA

ARTICLE INFO

Keywords:
Headward erosion
Recession
Mechanical stratigraphy
Fracture
Toppling
Undercutting
Spillway

ABSTRACT

This study investigates the role of mechanical layering and fractures on flood-related erosional undercutting and resulting rapid spillway recession. In the summer of 2002, 86 cm of rain fell in an 8-day period across the Guadalupe River drainage basin in central Texas, causing Canyon Lake reservoir to completely fill and overtop the emergency spillway for the first time. The resulting flood incised a gorge into the mechanically layered Glen Rose Formation and caused headward erosion (recession) at the downstream edge of the emergency spillway. Comparison of pre- and post-flood imagery and assessment of flood records indicates that maximum recession localized at the northern end of the emergency spillway where 28 m recession occurred. This recession occurred at an estimated rate of up to 10 m/day during the first ~3 days of the flood, which is among the highest rates of recorded bedrock recession. Analysis of historical photographs, field observations and measurement of erosional undercutting, along with measurements of fracture orientation, fracture spacing, and mechanical rebound are used to understand rock mass characteristics that influenced erosional undercutting and rapid recession of the spillway. Evidence of significant undercutting was observed where incompetent argillaceous wackestone (marl) underlies competent limestone. These results reveal that the greatest amount and rate of recession of the spillway was associated with undercutting and toppling collapse of fracture-bounded limestone blocks. Block size may be a factor in continuation of the process, in that large blocks may accumulate at the base of the scarp and inhibit continued erosional undercutting, whereas in other areas smaller eroded blocks can be carried away by the floodwaters and undercutting may continue, facilitating recession. The combination of mechanical contrast between layers and natural fractures in competent layers together contributed to exceptionally high rates of headward erosion. Observed rock mass erodibility behavior was in the range of medium to high erodibility in limestone with widely spaced fractures that would normally be expected to have very low erodibility. Bulk rock mass erodibility in this situation was similar to the most erodibile layer, specifically, the marl at base of spillway pour-off cliff.

1. Introduction

Understanding and mitigating erosional hazards requires detailed understanding of erosion processes and contributing factors. Common mechanisms of stream erosion include: abrasion – the process of wearing away by scraping or impacting of fluvially transported particles against the substrate, and plucking – lifting or removal of blocks in a fractured rock mass by hydraulic power (Paola et al., 2009; Lamb et al., 2015). Plucking includes block removal by vertical entrainment, which typically leaves a depression or pothole in the channel floor, or block sliding or toppling at knickpoints where fractured blocks are unconstrained at their downstream margins (Dublinski and Wohl, 2013; Lamb et al., 2015; Li et al., 2016). Undercutting – erosion at the base of a cliff or headwall (waterfall) due to turbulence or removal of softer rock under harder rock leaving an overhang – can be an important factor for headward erosion or "recession" (Mandych, 1935; Holland and Pickup, 1976; Gardner, 1983; Levin, 1989; Bishop and Goldrick, 1992; Bennett et al., 2000; Stein and LaTray, 2002; Frankel et al., 2007; Hayakawa and Matsukura, 2009, 2010; Haviv et al., 2010; Admassu et al., 2012; Dublinski and Wohl, 2013; Scheingross and Lamb, 2017). Erosion at Niagara Falls and its headward migration or recession has been studied since the 1600's (see review by Tinkler, 1987), and has long been

* Corresponding author.
E-mail address: dferrill@swri.org (D.A. Ferrill).

https://doi.org/10.1016/j.enggeo.2020.105897
Received 25 March 2020; Received in revised form 5 October 2020; Accepted 1 November 2020
Available online 4 November 2020

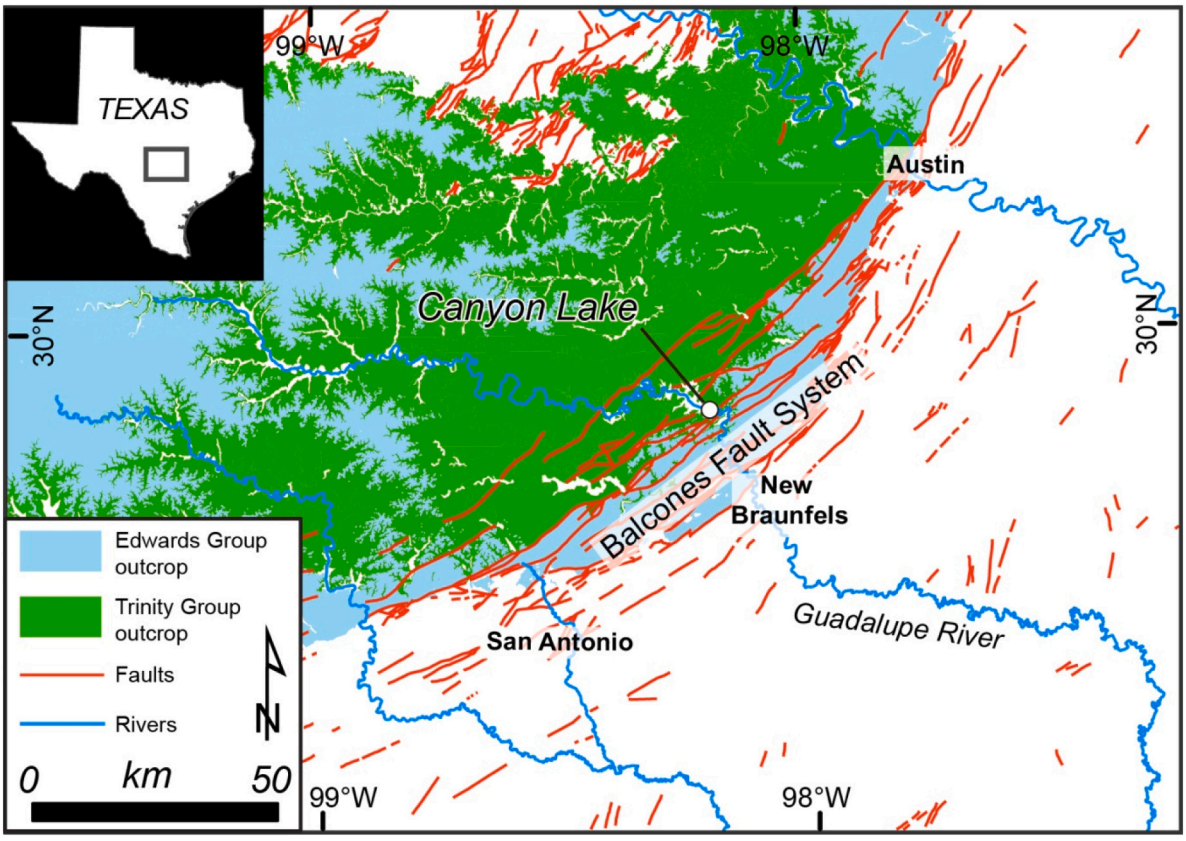

Fig. 1. Location of Canyon Lake gorge associated with the emergency spillway and Canyon Dam along the Guadalupe River in Central Texas, USA. Canyon Lake gorge was carved into the Cretaceous Glen Rose Formation, which constitutes most of the Trinity Group outcrop in the region shown in this map (Barnes et al., 1983; Collins, 2000). (For interpretation of the references to colour in this figure legend, the reader is referred to the web version of this article.)

considered a clear example of headward erosion by undercutting of an easily eroded stratum at the base of the falls and associated collapse (Gilbert, 1890, 1907). More recent work has provided further detail and support for the undercutting interpretation for Niagara Falls and the role of mechanical stratigraphy constrained by rebound measurements using a Schmidt rebound hammer – this work has, however, called into question the classic model of undercutting and collapse of the waterfall face (Hayakawa and Matsukura, 2010).

This project investigates the potential role of undercutting in the Glen Rose Formation at Canyon Lake gorge caused by the flood of 2002. In this paper, we investigate the role of undercutting in the uppermost Canyon Lake Gorge at the downstream edge of the unlined emergency spillway cut. We document evidence of erosional undercutting and headward erosion (recession) occurring at Canyon Lake spillway, and that this recession occurred at an extremely high rate. Characterization of mechanical properties of the eroded sequence using a Schmidt rebound hammer (e.g., Goudie, 2016), and assessment of natural fracturing and eroded blocks document important controls on the undercutting and recession process that has broad implications for understanding headward erosion (recession) in mechanically layered rocks. The study specifically addresses the interaction between geology and an engineered spillway, and documents an extremely high rate of headward erosion, and explores the causes of this erosion. This applied geomorphology and structural geology analysis represents a case history of potential interest and use by academic scientists, industry and applied researchers, and policy and decision makers. In particular, the rapid erosion rate of the fractured competent limestone is consistent with the erodibility of the underlying clay-rich marl, the weakest stratum in the section, rather than the lower erodibility of the cliff forming fractured limestone. This result is potentially relevant to assessing erodibility of other mechanically layered strata worldwide (e.g., Moosdorf et al., 2018) and at engineered facilities in mechanically layered strata (e.g., Nield, 2018). Results suggest that undercutting and block toppling or collapse was responsible for the most rapid recession of Canyon Lake's emergency spillway, providing a case example where mechanical stratigraphy and natural fracturing contribute to extreme recession rates and greatly enhanced rock-mass erodibility. We also show that the remaining undercut left by the flood has led to continued recession due to rockfall under non-flood conditions.

2. Study site

Canyon Lake dam was constructed on the Guadalupe River, 20 km north-northwest of New Braunfels, Texas (Fig. 1), from 1958 through 1964, and started to be filled in 1968 (Webb and Hull, 1962). The earthen dam was built to form a reservoir to control flooding of the Guadalupe River, supply water in times of drought, generate hydroelectric power, and for recreational purposes. The dam is 68 m high with an elevation of 297 m at the top of the dam and length of 1344 m with an emergency spillway south of the dam created to prevent water from flowing across the dam (Webb and Hull, 1962; Fig. 2a). The emergency spillway is founded on variably weathered and fractured Glen Rose Formation limestone, and includes an excavated 384 m wide unlined spillway (uncontrolled weir) cut into bedrock, an auxiliary dike installed at the south end of the uncontrolled weir to protect against erosion of a major normal fault zone (Hidden Valley fault, strike 057°, dip 60–70° SE, displacement 55–63 m, fault zone width ~ 100 m; Webb and Hull, 1962; Ferrill et al., 2011), and a concrete wall (right spillway training wall) against which the dike rests. The concrete structures of the right spillway training wall were pinned to the foundation with reinforcing bars grouted into holes drilled into bedrock (Webb and Hull, 1962). Curtain and fault consolidation grouting were performed under the

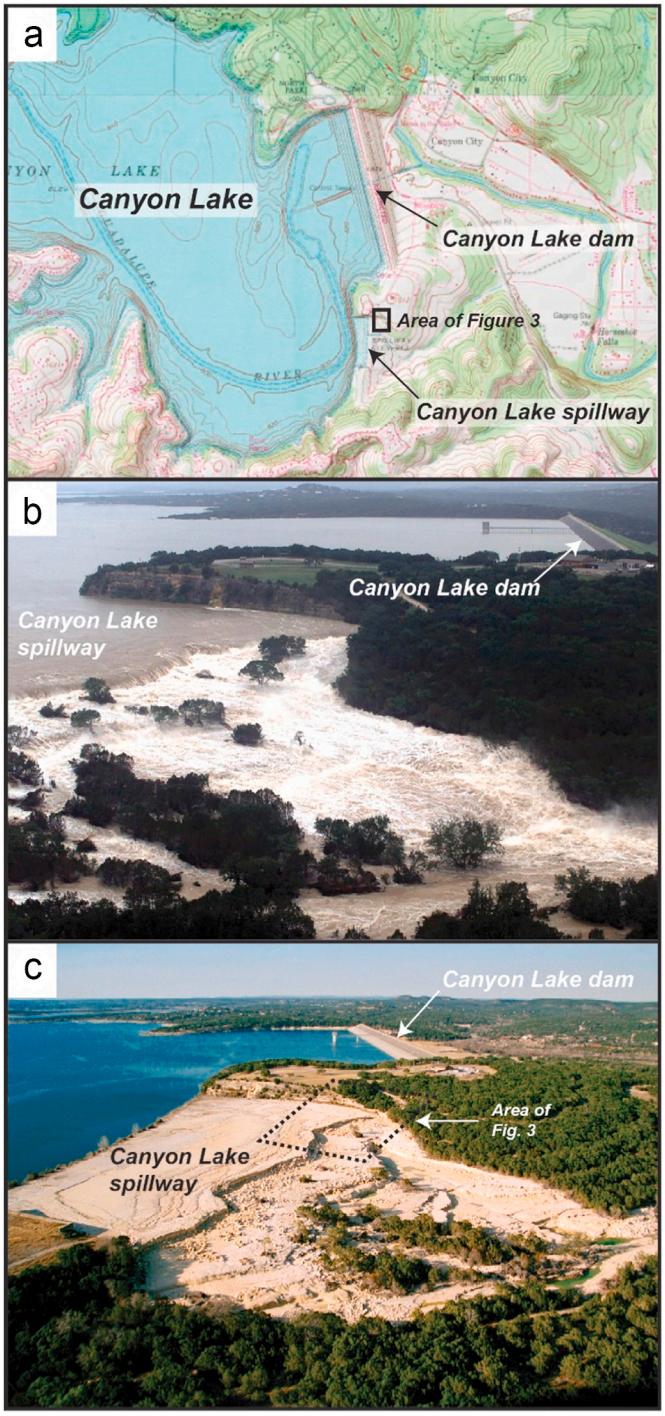

Fig. 2. (a) USGS topographic map of Canyon Dam on the Guadalupe River and spillway. (b) Photograph of Canyon Lake gorge during 2002 flood (photo credit, Comal County, Texas). (c) Photograph of Canyon Lake spillway and upper gorge on February 4, 2003.

auxiliary dike, under the right spillway training wall, and beneath the emergency spillway (Webb and Hull, 1962). The Canyon Lake emergency spillway fed into a vegetated valley with meadows and clusters of trees. Once the dam was completed, it took three years to fill the lake to the conservation pool level, and the emergency spillway never flowed water out of Canyon Lake until 2002.

In 2002, the Guadalupe River basin received 86 cm of rain from June 30 to July 3, 2002 (Lamb and Fonstad, 2010). The water level in Canyon Lake rose 10.4 m and began flowing across the 384 m wide emergency spillway for the first time on July 4, 2002 (Gorge Preservation Society, 2009; Lamb and Fonstad, 2010). At its peak, water 2.1 m deep rushed through the spillway at 1897 m^3/s (67,000 ft^3/s), versus the usual 10 m^3/s normally discharged through the dam and hydroelectric power plant (Fig. 2b). About 1½ times the water held in the lake on a normal basis went over the spillway during the flood. The flow through the spillway transformed a broad vegetated valley into a gorge carved into the bedrock with locally >12 m downward incision due to erosion (Fig. 2c), including excavating the Hidden Valley fault zone for an along-strike distance of 830 m which localized the deepest and narrowest portions of the bedrock gorge (Ferrill et al., 2011). This extraordinary event left a pristine erosional gorge that has provided a natural laboratory to study erosional processes (Lamb and Fonstad, 2010), stratigraphy (Ward and Ward, 2007), and faults and fracture networks revealed by the erosion (e.g., Ferrill et al., 2003; Ferrill and Morris, 2008; Ferrill et al., 2011; McGinnis et al., 2015).

Previous studies of stream erosion where there is distinctive mechanical layering often show evidence of major undercutting (e.g., Lamb et al., 2007; Lamb and Dietrich, 2009). An example of this process is Niagara Falls, New York, which is thought to have started flowing some 12,500 years ago and receded approximately 11 km (Gilbert, 1907; Tinkler et al., 1994; Hayakawa and Matsukura, 2009). Canyon Lake gorge formed during the 2002 flood within the mechanically layered carbonate stratigraphy of the Glen Rose Formation, with prominent steps and broad limestone pavements (Ward and Ward, 2007; Ferrill et al., 2011). The irregular and diverse topography in the eroded gorge (Fig. 2c) suggests multiple mechanisms of erosion were active in Canyon Lake spillway and upper gorge, potentially including erosional undercutting.

3. Methodology

3.1. Characterization of undercutting and headward erosion

A combination of field observations and analysis of ground photography, low-altitude oblique aerial photography taken within months after the flood, and Google Earth imagery was used to assess Canyon Lake spillway and upper gorge for evidence of erosional mechanisms and headward erosion. Research in Canyon Lake gorge by the research team began in September 2002 with on-the-ground field work in Canyon Lake gorge focused primarily on faults and fractures in the Glen Rose Limestone throughout the bedrock gorge. The earliest publication of this work was by Ferrill et al. (2003), but this research effort in the gorge has continued and is ongoing. Erosional undercutting of the uppermost spillway bench was observed (by D. Ferrill) immediately after the flood (September 2002). As part of the early work, the research team conducted a helicopter overflight on February 4, 2003 for the purpose of taking photographs and video of the newly formed gorge. These photographs taken soon after the flood provide an important dataset for this study. Video taken from helicopter and from the ground provide another important data source to understand flow behavior during the flood. In particular, Mr. Dan Cardenas, a local resident who shot video before, during, and immediately after the flood, graciously allowed us to duplicate and use his video. These images, along with observational field work, showed overwhelming evidence of undercutting of mechanically weak layer and overhangs of the interlayered fractured limestone at the downstream edge of the spillway. In addition, there was no evidence of potholes or depressions that are typically associated with plunge pools and substrate abrasion or plucking by vertical entrainment (e.g., Lamb et al., 2008; Scheingross and Lamb, 2017) or striations along the channel floor indicative of plucking by sliding. A combination of erosional undercut and toppled blocks, however, was observed along the upper spillway bench. Historical imagery in Google Earth provides another important data source that allows comparison of pre-flood and post-flood images that in particular constrain the position of the

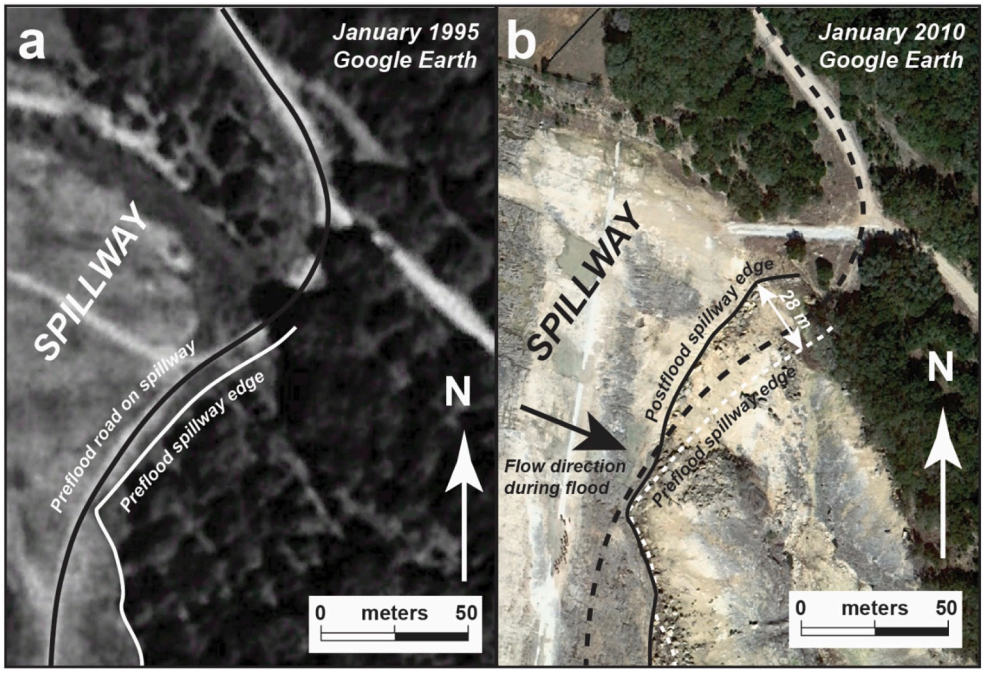

Fig. 3. Aerial imagery from Google Earth showing the spillway (a) before the flood (January 1995), and (b) after the flood (January 2010). Note that a road is visible on the north end of the spillway prior to the flood. Headward erosion (recession) along the downstream edge of the spillway produced 5 m to 28 m of recession along the northernmost 75 m of the spillway, removing a portion of the road.

downstream edge of the Canyon Lake spillway pre- and post-flood. In addition, comparison of post flood images allows for identifying occurrence and timing of post-flood rockfall. Field work was conducted to identify locations with evidence of erosional undercutting – recognized by overhanging cliff face at the downstream edge of the spillway – and quantify the amount of undercutting. The main field work specifically for this analysis was conducted in October 2015, October 2016, and October 2017.

3.2. Mechanical stratigraphy

The eroded scarp at the downstream edge of the emergency spillway is composed of lithologically diverse and mechanically variable strata, including a recessively weathered clay-rich marl layer at the base, overlain by more competent limestone beds. To characterize the mechanical stratigraphy where evidence of erosional undercutting and recession of the spillway was observed, we used a Schmidt rebound hammer to measure the in situ elastic rebound of the rock. Specifically, we used a type N Schmidt hammer (Katz et al., 2000; Aydin and Basu, 2005) for this rebound analysis, and followed the approach that was outlined in Morris et al. (2009) and Ferrill et al. (2011). Laboratory analysis of Schmidt rebound (R) versus other standard rock mechanical properties has demonstrated strong correlations of R to both unconfined compressive strength and Young's modulus (Katz et al., 2000; Aydin and Basu, 2005). Although mechanical rebound was previously measured and reported for the stratigraphic section at Canyon Lake gorge (Ferrill et al., 2011), new rebound analysis was performed in the focus area for this study where erosional undercutting was observed to document mechanical stratigraphy specific to this study location at a finer bed scale than the data reported by Ferrill et al. (2011). Each of the measurement locations was characterized using 10 Schmidt hammer strikes, and all measurements were made on subvertical rock surfaces so that no correction would be needed to correct for variations induced by gravity. Each measurement was made from a new location within the interval being tested with the objective of capturing natural variability of rock strength within each measured interval, following the approach of Katz et al. (2000) and Aydin and Basu (2005). Measurement at locations separated by a minimum of one plunger diameter between measurement locations is intended to ensure that the measurement is of undamaged rock (Katz et al., 2000), and to avoid strengthening (Aoki and Matsukura, 2007) or weakening behavior that can result from repeated measurement on the same location (Aydin and Basu, 2005). In making the measurements, we identified relatively unweathered limestone surfaces to measure, and for marl intervals, we were able to scrape through the weathered rind using a rock hammer to expose fresh rock from which measurements were made. The resulting data are summarized using a rebound, R, profile based on the measured thicknesses in the field, and average rebound measurements (mean of 10 measurements) from each measured interval.

3.3. Fracture orientation and spacing in competent headwall layer

Field observations revealed that the eroded outcrop faces in limestone beds in the eroded cliff edge at the downstream edge of Canyon Lake spillway are represented by fracture faces. These fracture surfaces typically exhibit calcite mineralization or iron-oxide staining – these characteristics were observable immediately after the flood and are indicative of the fractures having been present prior to the flood of 2002. These pre-existing fractures define eroded block-bounding surfaces, and therefore are likely to have been important factors during flood related erosion.

To constrain the fracture network, we measured representative fracture orientations (strike and dip) for observable systematic fracture sets in the emergency spillway cliff (headwall). For reporting measurements, we use the right hand rule where the dip is downward to the right of the reported strike. For each systematic fracture set, fracture-normal spacings between fractures were measured and recorded. From these data, mean and standard deviation, and maximum and minimum values were calculated using orientation (strike, dip) and spacing data for each fracture set.

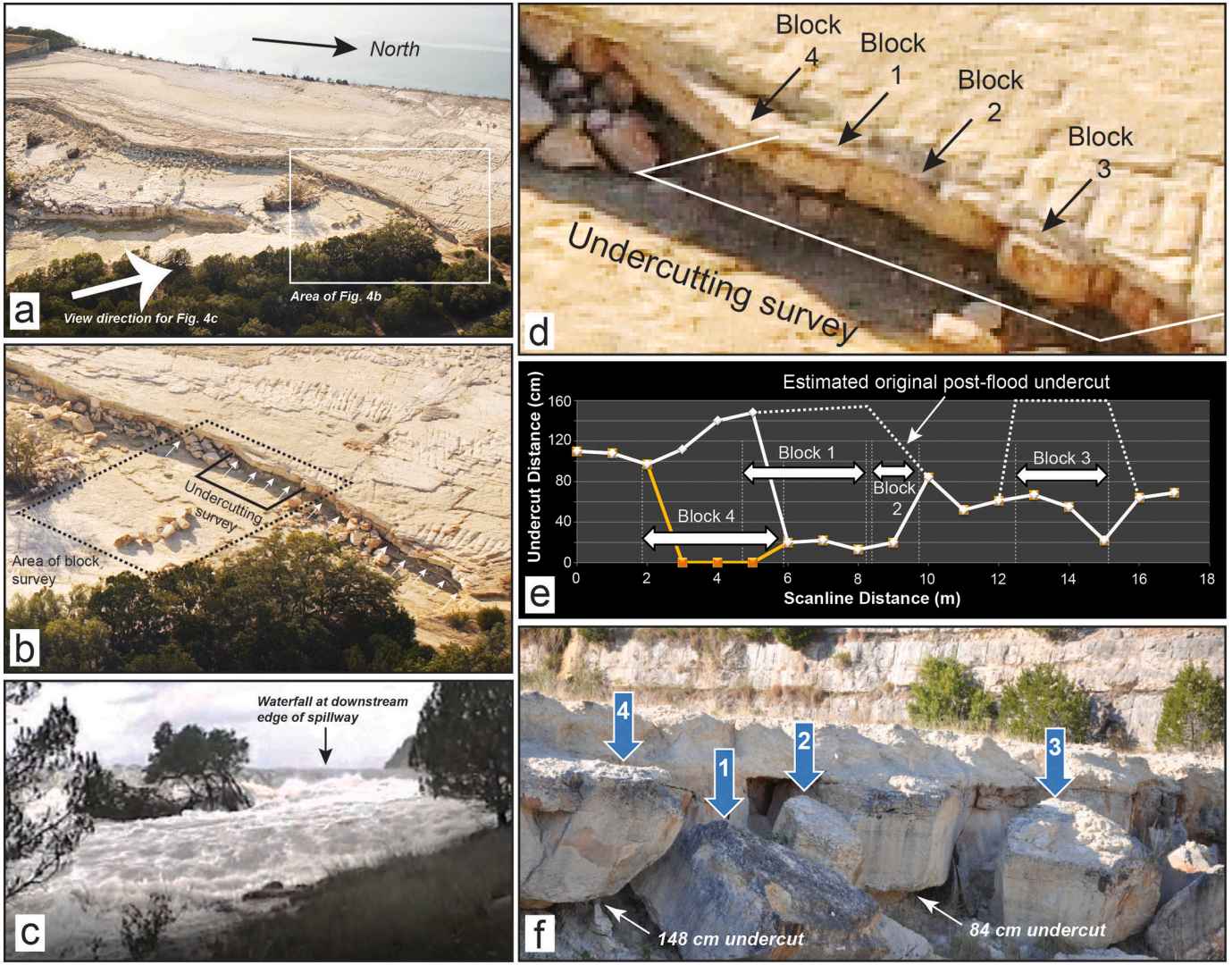

Fig. 4. (a) Photograph taken February 4, 2003, illustrating spillway and the eroded scarp at the downstream edge of the spillway. (b) Enlargement of part of the photograph in (a) where undercutting is visible along the scarp, as well as eroded blocks accumulated at the base of the scarp, and an elongate train of boulders along the pavement below the eroded scarp. (c) Image captured from video taken by Dan Cardenas in July 2002 during flood conditions. The waterfall noted in the image corresponds to the section of the spillway edge that is shown in Fig. 4b – note intense turbulence at the base of the falls, where undercutting occurred. (d) Further enlargement of photograph (b) detailing post-flood undercutting. Note this photo illustrates blocks 1–4 had large undercuts pre-collapse. (e) Profile illustrating undercut distance measured along a scanline parallel to the small scarp, with measurement spacing of 1 m. Undercutting was observed in marl at the base of the massive limestone in the cliff. Maximum undercutting of 1.5 m recorded in October 2015 (white line on graph) was site of collapse of Block 4 in 2016, with gold line illustrating the resulting undercutting profile. (f) Photo October 5, 2015 at time of original undercutting measurements, prior to the fall of Block 4. (For interpretation of the references to colour in this figure legend, the reader is referred to the web version of this article.)

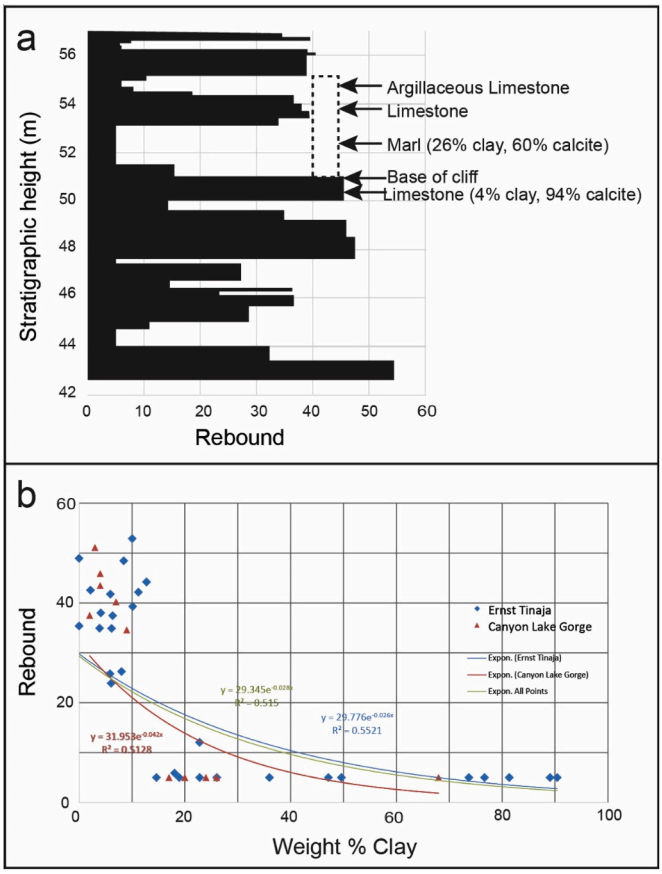

Fig. 5. (a) Schmidt rebound profile for the eroded upper spillway at Canyon Lake emergency spillway, including the eroded spillway cliff section. (b) Plot of rebound versus percent clay including data from the Glen Rose Formation at Canyon Lake gorge (Ferrill et al., 2011) and Boquillas Formation at Ernst Tinaja in Big Bend National Park, west Texas (McGinnis et al. (2017) shows an inverse correlation of increasing clay to decreasing competence. A major step change in behavior occurs at 15% clay. An exponential best-fit line is statistically significant, with R-value of 0.515. (For interpretation of the references to colour in this figure legend, the reader is referred to the web version of this article.)

3.4. Eroded block dimensions and orientations

Eroded blocks are present at the base of the cliff and scattered across the eroded bedrock pavement (top of competent limestone at the top of bed 51.0 in the measured section; Ward and Ward, 2007; Ferrill et al., 2011) below the cliff, the mapped area of which is referred to as Area 51 in Ferrill et al. (2011). For comparison with the strata and fracture networks exposed in the eroded spillway cliff edge – and adjacent to the area of headward erosion and measurements of erosional undercutting, fractures, and mechanical stratigraphy – eroded blocks were studied throughout a delineated 30 m × 30 m area. Within this area that is 30 m long parallel to the eroded cliff, and 30 m perpendicular to the eroded cliff, each eroded block that has at least one dimension ≥50 cm was measured and recorded. For each block, the median length, width, and thickness were measured, as well as the location of each block using a hand-held GPS. Using key stratigraphic markers – including limestone texture and a distinctive burrowed zone at the top of the most competent limestone bed (stratigraphic height 53.2–54.5 m) – a determination was made regarding whether each block was right side up or upside down, and bedding orientation was measured within each block and recorded as orientation upright versus overturned, and general dip (gentle, moderate, steep, vertical). In addition, observations were made to assess and record origin of block boundaries (e.g., lithologic partings vs. fracture and fracture type).

4. Results

4.1. Characterization of undercutting and headward erosion

Comparison of pre-flood and post flood imagery in Google Earth reveals that the downstream edge of the spillway, although eroded by the flood, did not experience major recession except for the northernmost approximately 75 m of the spillway. In pre-flood imagery of this area (Fig. 3a), an unpaved access road is visible between trees and continuing onto the emergency spillway surface. After the flood, the portion of the road on top of the spillway has been removed by recession of the spillway, and the access road between trees is abruptly truncated by the eroded cliff produced by the headwardly eroded gorge (Fig. 3b). Comparing the downstream edge of the spillway surface before (Fig. 3a) and after (Fig. 3b) the flood of 2002 shows that 5 m to 28 m of recession occurred during the flood of 2002 along the northern 75 m of the spillway. Maximum recession of 28 m occurred at the northern edge of the spillway.

Undercutting was observed in argillaceous packstone and wackestone (clay rich marl) between the stratigraphic heights of 51.0 m and 53.2 m (Fig. 4a). Undercut distance was measured along a 17 m scanline parallel to the scarp where the section from the spillway to near the base of the cliff was accessible (i.e., not covered by eroded blocks; Fig. 4b). This undercut was created predominantly during the 2002 flood (Fig. 4c), leaving unsupported limestone blocks throughout the study site (Fig. 4d). Undercut distance measurements were made horizontally, with measurement spacing of 1 m. Maximum undercutting of 1.48 m was initially recorded in October 2015, which is illustrated by the white line on the graph in Fig. 4e. Upon revisiting the following year – October 2016 – we found that this location was the site of toppling collapse of a block (labelled Block 4 in October 2015 photo in Fig. 4f). The gold line in Fig. 4e illustrates the updated undercutting profile after that rockfall/toppling event, and the dashed white line represents estimated original post-flood undercut (see photograph in Fig. 4d).

4.2. Mechanical stratigraphy

Rebound measurements were made horizontally against vertical outcrop surfaces (10 measurements per interval) and averaged to determine mean rebound for each bed within the section exposed in the eroded cliff at the downstream edge of the spillway. In making the measurements, we were able to find relatively unweathered limestone surfaces to measure on, and in weathered marl intervals, we were able to scrape through the weathered rind using a rock hammer to expose fresh rock to measure from. A rebound profile was generated using mean rebound values and interval thicknesses measured in the field (Fig. 5a). Average rebound values range from 5.0 in the clay-rich marl (packstone and wackestone) at the base of the cliff, to 39.4 in the overlying thick limestone bed that represents the dominant competent layer in the eroded cliff. To assess whether rebound values have changed significantly over time, we compare our new rebound measurements to rebound data collected from this section in 2008, 6 years after the flood of 2002, and published in Ferrill et al. (2011). Measurements for the

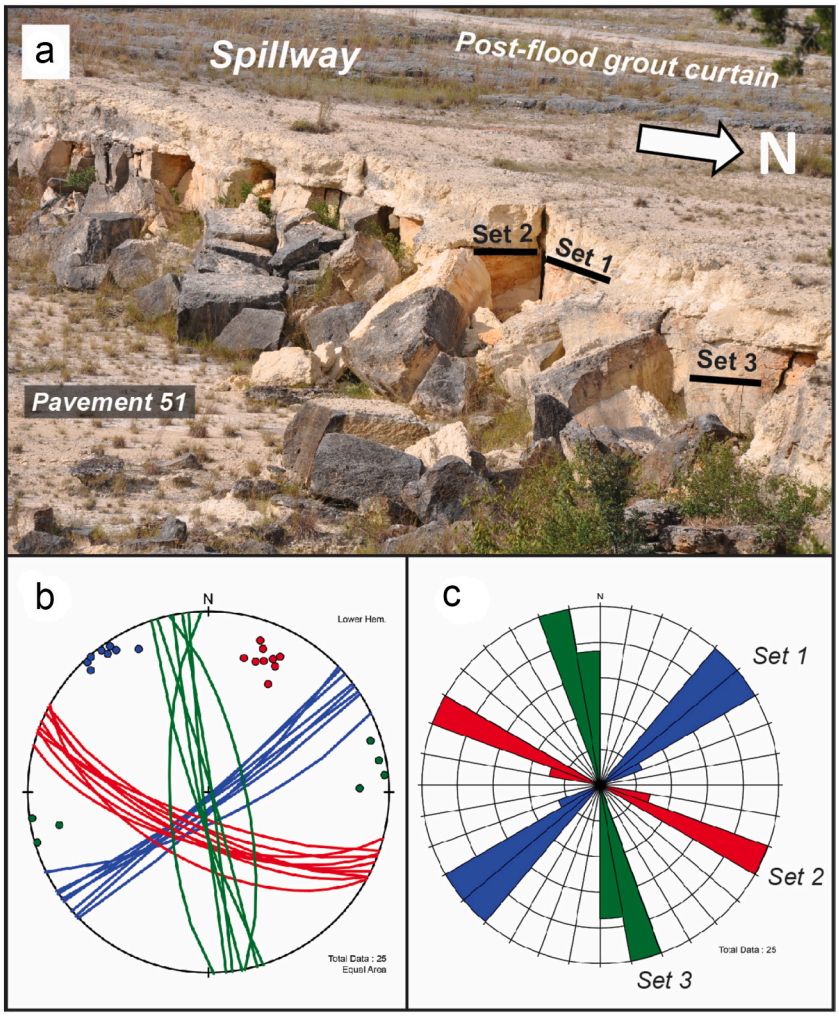

Fig. 6. (a) Field photograph (October 2016) showing fractures along downstream edge of spillway. (b) Equal area stereographic projection illustrating poles (dots) and great circles for measured fractures of each of the three systematic fracture sets. (c) Rose diagram illustrating the strike of fractures in each set. Set 1 (Blue) = 51.38° ± 3.9°; Set 2 (Red) = 113.75° ± 4.57°; Set 3 (Green) = 169.17° ± 5.49°. (For interpretation of the references to colour in this figure legend, the reader is referred to the web version of this article.)

present study were collected with a finer bed scale – in the present study we collected Schmidt rebound measurements for 12 distinct bed intervals at stratigraphic heights between 51.0 and 55.15, whereas Ferrill et al. (2011), in their rebound profile that represents the entire 97 m stratigraphic section exposed in Canyon Lake gorge, represented this interval as 4 mechanical layers. Comparing the 2008 measurements shows that the strength of the weakest material has remained below the measurement resolution of the Schmidt hammer (i.e., <10), and the strongest interval measured at stratigraphic height 53.5 had an average rebound of 39.4, whereas this interval is represented as 38.5 in Ferrill et al., (2011), showing retention of strength over that time period.

4.3. Fracture orientation and spacing in competent headwall layer

Three systematic fracture sets were identified in the headwardly eroded emergency spillway cliff (Fig. 6a). Orientations were measured for each set, and average strike/dip and spacing were calculated as follows: (i) Set 1–051/86, mean spacing 77 ± 70 cm; (ii) Set 2–114/68, mean spacing = 152 ± 90 cm; and (iii) Set 3–169/82, mean spacing = 256 ± 70 cm (Fig. 6b, c). The 051/86 fracture set is the dominant regional fracture set, and parallels the strike of the Hidden Valley fault exposed in Canyon Lake gorge and the dominant normal fault strikes in the Balcones fault zone in the region more broadly (Ferrill et al., 2011; McGinnis et al., 2015; Fig. 1). It is also noteworthy that Set 1 fractures parallel the pre-flood spillway edge in the north end of the spillway, and are normal to the flow direction and represent the primary release planes for block toppling and rockfall.

4.4. Eroded block dimensions and orientations

Dimensions and orientations of 63 blocks were characterized (within the 30 m × 30 m block survey area) below the eroded and undercut cliff. These blocks include 41 blocks that were present soon after the flood (February 4, 2003; Fig. 4b), and 22 additional blocks that formed by collapse of the undercut scarp after February 4, 2003. Eroded block thicknesses, measured perpendicular to layering, range from 10 cm to 131 cm, and average 70.2 cm. Block length (bed-parallel long dimension) measured parallel to layering through the middle of the blocks range from 40 cm to 363 cm, and average 115.0 cm. Block widths measured parallel to layering through the middle of the blocks, and perpendicular to bed-parallel long dimension, range from 3 cm to 292 cm, and average 69.8 cm.

Block tilt with respect to initial horizontal and upright orientation, was determined from bedding orientation within blocks and right-way-up indicators including a distinctive burrowed layer at the top of the massive limestone. Some blocks have tilted less than 90 degrees and therefore remain upright with bedding ranging from nearly horizontal to vertical. Other blocks have toppled over and are now overturned such

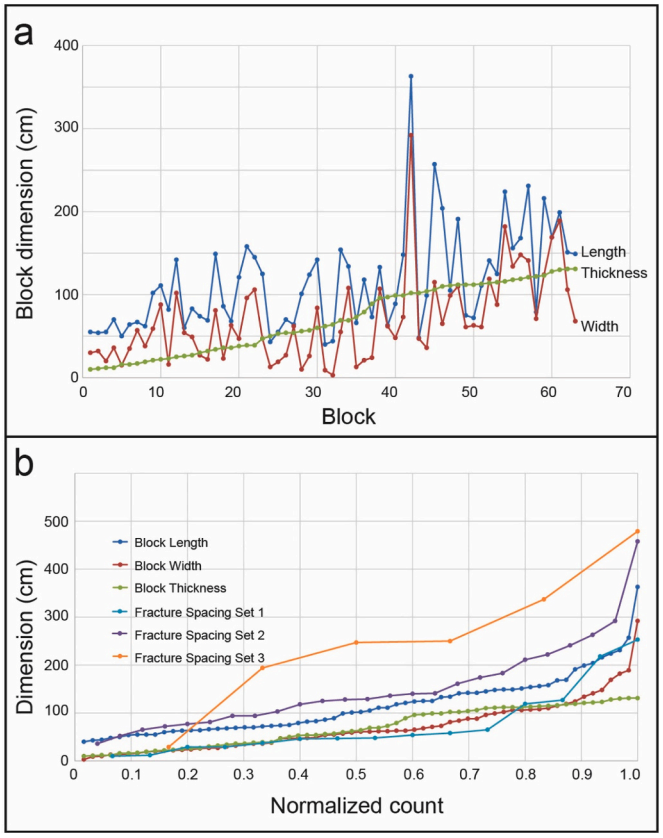

Fig. 7. (a) Graph of block dimension values vs block number ordered according to thickness dimension. (b) Graph of block dimension values vs normalized count showing that natural fracture spacings generally bracket the block dimensions. Whereas block thickness is controlled by mechanical layer thicknesses, length and width of blocks is determined by pre-existing fracture spacings.

that the stratigraphic "up" or younging direction now points downward. Of the 63 blocks analyzed, 12 lie horizontal and upright, 41 are gently inclined to vertical and upright, and 10 are overturned. These observations clearly indicate the common occurrence of block toppling. However, the largest eroded block (363 cm × 292 cm × 102 cm thick) in the survey area remains upright – this block may have essentially dropped in place during erosional undercutting and scouring during spillway recession while other smaller nearby blocks were transported away down the gorge by flood currents.

A graph of block dimensions – including thickness, length, and width for the 63 blocks ordered by thickness – illustrates the limited thickness range from 10 to 131 cm (Fig. 7a). In contrast, length and width show much greater variability. Maximum block thickness is controlled primarily by the relatively uniform mechanical layer thickness for the dominant competent limestone bed including the burrowed top (stratigraphic height 53.2 to 54.5 m). In contrast, the highly variable lateral dimensions of blocks are a function of the variable natural fracture spacing for each of the fracture sets that can in combination lead to a wide range of lateral dimensions. Plotting the three block dimensions as well as spacing for the three fracture sets on a graph of dimensions versus normalized count shows that natural fracture spacings generally bracket the block dimensions, supporting the interpretation that lateral block dimensions are controlled by pre-existing fractures (Fig. 7b).

Between October 2015 and October 2016, a new rockfall occurred (Fig. 8a, b). The rockfall occurred (Fig. 8b) where maximum undercutting of 148 cm was measured and documented during field research the previous year (Fig. 8a). Based on analysis of Google Earth historical images, the block toppled between February and October 2016. This new block (Fig. 8b) is bounded by fractures on lateral sides, and bedding partings/weaknesses on top and bottom. Block bounding fractures are not newly formed, but instead exhibit mineralization that indicates they are pre-existing natural fractures that reactivated (Fig. 8a). Lateral block boundaries are represented by fractures including both opening mode fractures with calcite mineralization, and minor shear fractures ornamented with slickenlines. The top of the block is defined by the distinctive burrowed layer, and the overlying argillaceous limestone sheared off and is now represented by smaller blocks and rubble (Fig. 8b).

5. Discussion

Pre-existing fractures and mechanical layering both contributed to erosion of the scarp via undercutting. This headwall is nearly vertical with a stronger limestone sitting above a weaker clay-rich marl layer (argillaceous packstone and wackestone), representative of the alternating mechanical layers that make up the Glen Rose Formation (Ward and Ward, 2007; Ferrill et al., 2011). Field observations and review of early post-flood photographs document significant undercutting along the spillway cliff, especially well developed in the area where maximum recession of the spillway occurred during the flood. Analysis of this area documents that undercutting occurred in weaker clay-rich marl beneath more competent limestone, and that large blocks toppled out due to undercutting, making it a prominent erosional process during the erosion in the uppermost Canyon Lake gorge (Fig. 4). Although local trains of eroded blocks are present downstream of eroded scarp left behind during spillway recession, most of the blocks were transported by floodwater down the gorge (Fig. 4a,b).

Undercutting and toppling associated with erosion at Canyon Lake gorge has been strongly influenced by mechanical layering and the pre-existing natural fracture network. Analysis of the mechanical layering using the Schmidt (type N) rebound hammer revealed dramatic contrast within the eroded emergency spillway section, with undercutting focused along the weakest layer in the section (Fig. 5a). A comparison of rebound versus weight percent clay from XRD whole-rock mineralogy data sets collected from the Cretaceous Glen Rose Limestone at Canyon Lake gorge (Ferrill et al., 2011) along with data from the Cretacous Boquillas Formation (limestone, chalk, carbonate mudrock) in Big Bend National Park (McGinnis et al., 2017) shows a strong relationship between increasing clay content and lower rebound (i.e., weaker rock) (Fig. 5b). Specific to this study, clay content is 26 wt% sampled from stratigraphic height of 52.8 (rebound = 5), whereas the underlying limestone has 4 wt% clay sampled from stratigraphic height = 50.8 (rebound = 45.9). It is apparent that clay content is a primary control on rock strength and erodibility in carbonate strata. Rock mechanical properties alone do not, however, control the headward erosion process. Whereas clay rich strata are not prone to brittle fracturing, competent limestone has low ductility and does commonly contain natural fractures (Ferrill et al., 2014; McGinnis et al., 2015, 2017). These fractures are a key contibutor to the headward erosion observed from Canyon Lake spillway.

Headward erosion or the recession process follows a recurring sequence. Based on observations and data gathered at Canyon Lake gorge, a conceptual erosion model specific to this study site is presented (Fig. 9). The first step of the erosional process initiates with water traveling downstream and flowing over the cliff at the downstream edge

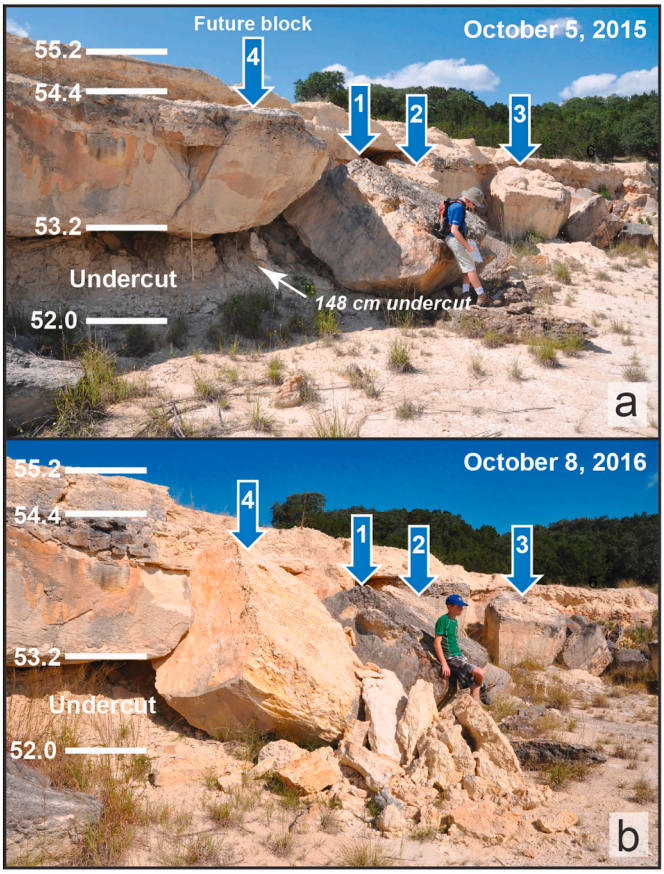

Fig. 8. Toppling failure continues, associated with erosional undercut. (a) Photograph taken October 5, 2015, with several toppled blocks identified. (b) Photograph from the same location taken October 8, 2016 shows a newly toppled block (4). Rubble at the bottom of block 4 represents relatively weak argillaceous limestone from stratigraphic height 54.4–55.2 that sheared off the top of the toppled block.

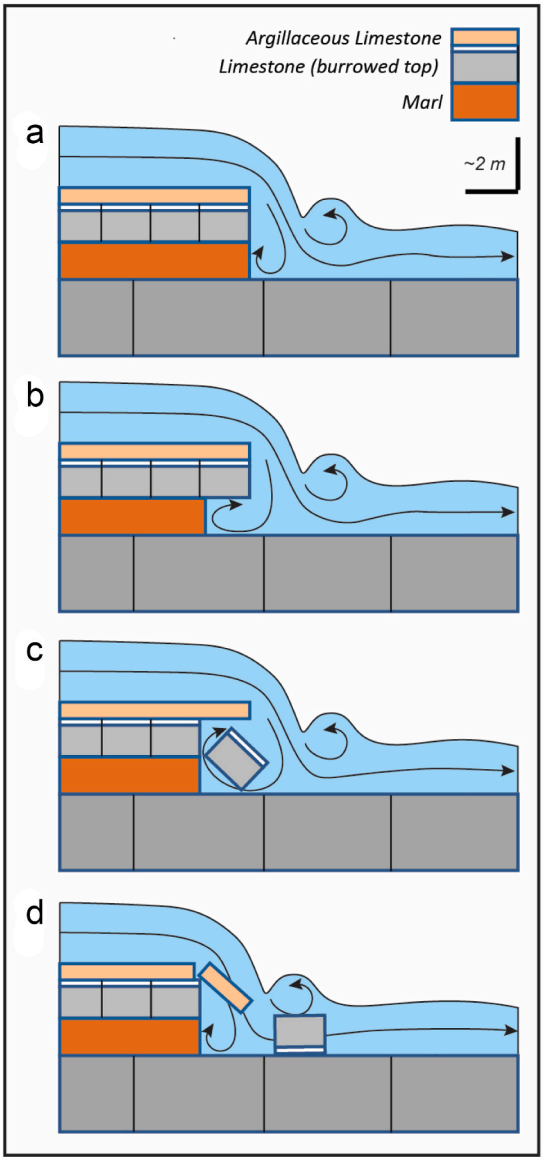

Fig. 9. Model for sequential undercutting and block toppling in mechanically layered limestone and marl. Erosion of weak marl at base of waterfall undercuts beneath limestone which progressively destabilizes fractured limestone and leads to blocks toppling out of cliff, and collapse progressing to the top of the cliff. This process repeats as eroded blocks are transported by current downstream and marl continues to undercut at base of cliff.

of the spillway (Fig. 9a). This water entrains sediment that impacts and recirculates at the bottom of the cliff, forming an erosional vortex current that scours or abrades the softer clay-rich marl layer causing erosion. Next, continued erosion of the clay-rich marl produces undercutting of the overlying erosionally resistant limestone (Fig. 9b). Continued erosional undercutting leads to the marl becoming eroded enough to expose or reactivate fractures in the overlying limestone layer. In this case, the flow is perpendicular to the dominant regional fracture set (Set 1), and these fractures serve as the primary release planes for blocks to topple or collapse from the waterfall headwall (Fig. 9c). The fourth step in the erosional process is the failure of the unstable marl above the limestone due to overhang and mechanical weakness – this may occur during collapse of the underlying limestone block or be delayed during progressive collapse (Fig. 9d). After collapse of the cliff, renewed erosion of the clay-rich marl catalyzes undercutting and the process repeats.

Observations presented here indicate fundamental influence of pre-existing fractures on recession along the waterfall lip at the Canyon Lake spillway. This is consistent with the results from past erosion studies and analysis methods (e.g., Annandale, 2005; Pan et al., 2014), and of Bishop and Goldrick (1992) that indicated that failure along joint planes at waterfall lips enhances retreat as part of a more complicated process than the simple model for undercutting beneath a competent caprock layer that has been interpreted for Niagara Falls. Erodibility has been defined as the relationship between the velocity of the water flowing over the soil or rock and the corresponding erosion rate experienced by the soil or rock (Briaud, 2008; Briaud et al., 2008). Briaud et al. (2008) notes that rock erodes through two main processes of rock substance erosion and rock mass erosion, with the distinction that rock mass erosion involves removal of rock blocks from a jointed rock mass which is particulary important for high turbulence events. The erodibility of the north end of Canyon Lake spillway can be evaluated through comparison with erodibility analyses of Briaud, (2008) and Briaud et al. (2008). Erosional recession rate at the north end of the spillway was 56 to 417 mm/h (based on 5 to 28 m recession occurring over 2.8 to 3.7 days) and 2.35 m/s velocity (1897 m^3/s peak discharge divided by 2.1 m water depth and 384 m width of emergency spillway) (Fig. 10). On a graph of erosion rate versus velocity (after Briaud, 2008), the erosion rate observed at Canyon Lake spillway plots in the area of medium (to high) erodibility (Fig. 10), which would typically be associated with unlithified clay, sand, or gravel, or intensely fractured rock with joint spacing <3 cm. In contrast, the limestones in the spillway cliff have mean joint spacings of 77 cm, 252 cm, and 256 cm, which according to Briaud et al. (2008) should be expected to have very low erodibility and would be expected to experience erosion at the observed recession rates only at flow velocities two orders of magnitude higher than the actual flow velocity. Although the jointed limestone in isolation would be expected to have very low erodibility according to Briaud et al. (2008), the greater erodibility of the underlying marl – with behavior similar to low-pasticity clay – led to undercutting of the limestone and "medium erodibility" of the composite section.

Accumulation of large blocks that are too large to be transported by the current may armor the scarp and inhibit undercutting or block toppling or fall. Previous work has shown that downstream transport of eroded blocks can be rate-limiting with respect to erosion by plucking (Howard, 1994; Lamb et al., 2015). This may partially explain why the entire spillway did not experience the magnitude of recession experienced by the north end of the spillway. The rapid decline in discharge from the spillway essentially preserved a fossil waterfall at the downstream edge of the spillway. After the flood, the undercut cliff was preserved, and eroded blocks were left stranded by the waning flow. Some of the largest blocks may have been stranded during peak flood due to inability of the current to transport these blocks, while smaller clasts were transported down the gorge. In the final stages, small clasts eroded during diminishing flow were trapped by larger blocks or in eddy currents or otherwise stranded due to insufficient current transport capacity.

Post-flood erosion by rockfall continues and has locally produced an additional 1 to 2 m of post flood recession, primarily associated with collapse where pronounced undercutting at the base of the spillway cliff was preserved at the end of flood (Fig. 11a), and through time blocks have collapsed (Fig. 11b). Toppling failure and rockfall has continued well over a decade after the flood, including the toppling of Block 4 between February and October 2016, which was described and documented before and after the rockfall. Observations of this ongoing

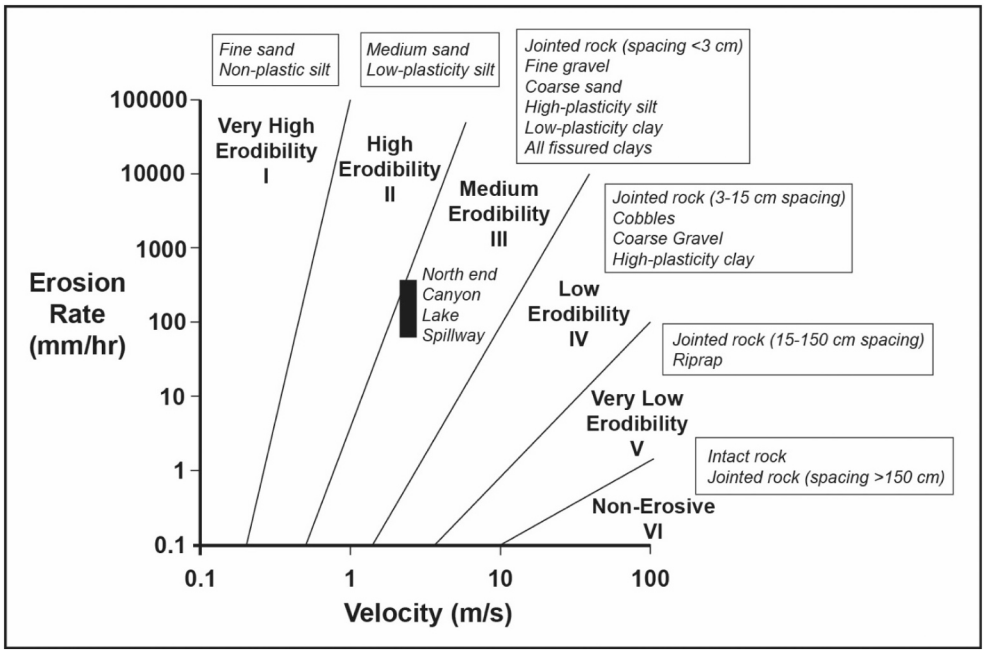

Fig. 10. Erosion rate versus water flow velocity at the north end Canyon Lake spillway is compared with erodibility of common geological materials including unlithified sediments and fractured bedrock. While competent limestone layers with fractures spaced more widely than 15 cm would typically lie between regions V – Very Low Erodibility and VI – Non-Erosive, the erosion of the limestone layers in the spillway at Canyon Lake plots in the region II – High erodibility to III – Medium Erodibility. This behavior is governed by the erodibility of the underlying marl, which behaves similarly to low-plasticity clay, and localizes undercutting to catalyze collapse of fracture bounded limestone blocks.

rockfall represent slower headward erosion during non-flood conditions.

Measured headward erosion based on pre- and post-flood aerial images indicates that the scarp eroded back as much as 28 m during the 2002 flood. Assuming most of this erosion occurred in 2.8–3.7 days as interpreted by Lamb and Fonstad (2010), recession occurred at a rate of 7.6 to 10.0 m/day, or 315 to 417 mm/h. For comparison, Briaud et al. (2008) cites that the long-term average rate for 11 km recession of Niagra Falls is 0.1 mm/h. Other published long-term rates of natural waterfall headward erosion or recession range from approximately 1 mm/yr up to <2 m/year, as discussed by Hayakawa and Matsukura (2009). These published rates of recession were found to be influenced by annual drainage volume (drainage area × precipitation), waterfall dimensions (width, height), and unconfined compressive strength of the bedrock. The much higher maximum rate of of 7.6 to 10.0 m/day presented here for the Canyon Lake emergency spillway represents a single brief event, and also a first event of significant flow across this mechanically layered, fractured, and weathered bedrock section. A steel-reinforced grout curtain was installed by the U.S. Army Corps of Engineers after the flood. This grout curtain was constructed in a trench cut deep enough to continue through the weak layer that localized the undercutting during the 2002 flood to protect against future headward erosion of the spillway.

From our work, we conclude that erosional undercutting and block toppling were principal mechanisms of headward erosion (recession) of the north end of the Canyon Lake emergency spillway during the flood of 2002. Recognition of this undercutting, and understanding the contributing factors of mechanical stratigraphy and fracturing, are particularly significant from an engineering geology perspective as this erosion caused extremely rapid recession of the spillway. The fundamental influence that the combination of mechanical stratigraphy and natural fracturing has to increase the overall rock mass erodibility is of particlular importance for siting of spillways or other erosion-sensitive drainage structures.

6. Conclusions

The Canyon Lake gorge flood of 2002 produced undercutting along the emergency spillway, which was localized by relatively incompetent clay-rich marl beneath naturally fractured competent limestone. This undercutting strongly contributed to recession of the downstream edge of the emergency spillway. Comparison of the pre- and post-flood imagery shows that the greatest amount of headward erosion occurred at the north end of the spillway where 28 m of headward erosion occurred during the previously reported 2.8–3.7 days of high discharge through the spillway. Maximum headward erosion occurred at a rate of 7.6 to 10.0 m/day. Headward erosion is continuing at a low rate, due to the instability of the rock face related to significant fracturing and the overhang due to erosional undercutting in the underlying clay-rich marl left behind after the flood.

Mechanical layering and natural fracture networks produce structural weaknesses within a stratigraphic section that can enable undercutting and rapid recession. Eroded block thickness is controlled by mechanical layer thickness, and lateral dimensions are controlled by natural fracture spacing. The largest eroded blocks are bounded by widely spaced fractures. Large blocks may be too large for transport by the floodwater, while smaller blocks are transported away by the current. Accumulation of oversized blocks – those too large for current to move – may conceivably armor a waterfall scarp and inhibit subsequent undercutting and rockfall/toppling erosion. The combination of mechanical contrast between layers and natural fractures in competent layers together contributed to exceptionally high rates of headward erosion, and rock mass erodibility behavior in the range of medium to high erodibility in limestone with widely spaced fractures that would normally be expected to have very low erodibility. These results provide a cautionary case study, illustrating the importance of the combination of mechanical stratigraphy and natural fracturing to enhance rock mass erodibility that is of broad relevance for erosion in mechanically layered rocks.

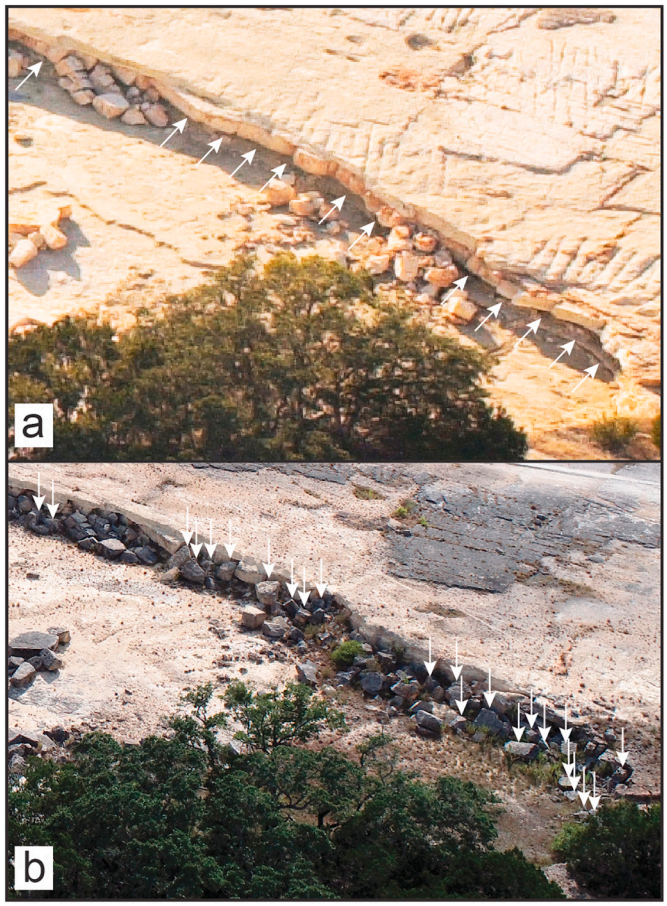

Fig. 11. (a) Photograph from February 4, 2003 illustrating post-flood undercutting along the scarp, indicated by white arrows. (b) Photograph from July 24, 2020 showing the collapse of 23 new blocks, indicated by vertical white arrows. Collapse of these blocks has led to locally 1–2 m of post-flood recession of the emergency spillway edge.

Declaration of Competing Interest

None.

Acknowledgments

We thank Jaynellen Kerr, the Gorge Preservation Society, and the Guadalupe Blanco River Authority for research access to Canyon Lake gorge, Larry Walther for the February 2003 photography of Canyon Lake gorge, and Adam Cawood for the July 2020 drone photography. We also thank Dan Cardenas for providing us with his video coverage of the formation of Canyon Lake gorge. This research did not receive any specific grant from funding agencies in the public, commercial, or not-for-profit sectors. The authors thank the four technical reviewers, and the handling editor for constructive comments that improved this manuscript.

References

Admassu, Y., Shakoor, A., Wells, N.A., 2012. Evaluating selected factors affecting the depth of undercutting in rocks subject to differential weathering. Eng. Geol. 124, 1–11.

Annandale, G.W., 2005. Scour Technology. McGraw-Hill New York, Mechanics and Engineering Practice, p. 420.

Aoki, H., Matsukura, Y., 2007. A new technique for non-destructive field measurement of rock- surface strength: an application of the Equotip hardness tester to weathering studies. Earth Surf. Process. Landf. 32, 1759–1769. https://doi.org/10.1002/esp.1492.

Aydin, A., Basu, A., 2005. The Schmidt hammer in rock material characterization. Eng. Geol. 81, 1–14.

Barnes, V.E., Brown, T.E., Waechter, N.B., Dillon, R.L., 1983. Geologic Atlas of Texas, San Antonio Sheet. Austin, University of Texas, Bureau of Economic Geology, Scale 1: 250,000, 1 Sheet.

Bennett, S.J., Alonso, C.V., Prasad, S.N., Römkens, M.J.M., 2000. Experiments on headcut growth and migration in concentrated flows typical of upland areas. Water Resour. Res. 36, 1911–1922.

Bishop, P., Goldrick, G., 1992. Morphology, processes and evolution of two waterfalls near Cowra, New South Wales. Aust. Geogr. 23 (2), 116–121. https://doi.org/10.1080/00049189208703061.

Briaud, J.-L., 2008. Case histories in soil and rock erosion: Woodrow Wilson Bridge, Brazos River meander, Normandy cliffs, and New Orleans levees. J. Geotech. Geoenviron. Eng. 134, 1425–1447. https://doi.org/10.1061/(ASCE)1090-0241(2008)134:10(1425).

Briaud, J.-L., Chen, A.V., Govindasamy, A.V., Storesund, R., 2008. Levee erosion by overtopping in New Orleans during the Katrina Hurricane. J. Geotech. Geoenviron. Eng. 134, 618–632.

Collins, E.W., 2000. Geologic Map of the New Braunfels, Texas, 30×60 Minute Quadrangle: Geologic Framework of an Urban-Growth Corridor along the Edwards Aquifer, 39. University of Texas at Austin, Bureau of Economic Geology Miscellaneous Map, South-Central Texas (28 p., scale 1:100,000, 1 sheet).

Dublinski, I.M., Wohl, E., 2013. Relationships between block quarrying, bed shear stress, and stream power: a physical model of block quarrying of a jointed bedrock channel. Geomorphology 180-181, 66–81.

Ferrill, D.A., Morris, A.P., 2008. Fault zone deformation controlled by carbonate mechanical stratigraphy, Balcones fault system, Texas. Am. Assoc. Pet. Geol. Bull. 92, 359–380.

Ferrill, D.A., Sims, D.W., Morris, A.P., Waiting, D.J., Franklin, N., 2003. Structural Controls on the Edwards Aquifer/Trinity Aquifer Interface in the Camp Bullis Quadrangle, Texas. Report for the Edwards Aquifer Authority and the U.S. Army Corps of Engineers, 126 p., https://www.edwardsaquifer.org/wp-content/uploads/2019/05/2003_Ferrill-etal_StructuralControlsCampBullisQuadrangle.pdf (last accessed July 26, 2020).

Ferrill, D.A., Morris, A.P., McGinnis, R.N., Smart, K.J., Ward, W.C., 2011. Fault zone deformation and displacement partitioning in mechanically layered carbonates: the Hidden Valley fault, Central Texas. Am. Assoc. Pet. Geol. Bull. 95, 1383–1397.

Ferrill, D.A., McGinnis, R.N., Morris, A.P., Smart, K.J., Sickmann, Z.T., Bentz, M., Lehrmann, D., Evans, M.A., 2014. Control of mechanical stratigraphy on bed-

restricted jointing and normal faulting: Eagle Ford Formation, south-Central Texas, U.S.A. Am. Assoc. Petrol. Geol. Bull. 98, 2477–2506.
Frankel, K.L., Pazzaglia, F.J., Vaughn, J.D., 2007. Knickpoint evolution in a vertically bedded substrate, upstream-dipping terraces, and Atlantic slope bedrock channels. Geol. Soc. Am. Bull. 119, 476–486. https://doi.org/10.1130/B25965.1.
Gardner, T.W., 1983. Experimental study of knickpoint and longitudinal profile evolution in cohesive, homogeneous material. Geol. Soc. Am. Bull. 94, 664–672.
Gilbert, G.K., 1890. The History of the Niagara River. James Lyon, Albany (84 pp).
Gilbert, G.K., 1907. Rate of recession of Niagara Falls, U.S. Geol. Surv. Bull. 306, 1–31.
Gorge Preservation Society, 2009. Canyon Gorge. Web. 10 May 2015. http://canyongorge.org/>.
Goudie, A.S., 2016. Quantification of rock control in geomorphology. Earth Sci. Rev. 159, 374–387.
Haviv, I., Enzel, Y., Whipple, K.X., Zilberman, E., Matmon, A., Stone, J., Fifield, K.L., 2010. Evolution of vertical knickpoints (waterfalls) with resistant caprock: insights from numerical modeling. J. Geophys. Res. 115, F03028. https://doi.org/10.1029/2008JF001187.
Hayakawa, S., Matsukura, Y., 2009. Factors influencing the recession rate of Niagara Falls since the 19th century. Geomorphology 110 (3–4), 212–216.
Hayakawa, S., Matsukura, Y., 2010. Stability analysis of waterfall cliff face at Niagara Falls: an implication to erosional mechanism of waterfall. Eng. Geol. 116 (1–2), 178–183.
Holland, W.N., Pickup, G., 1976. Flume study of knickpoint development in stratified sediment. Geol. Soc. Am. Bull. 87, 76–82.
Howard, A.D., 1994. A detachment-limited model of drainage basin evolution. Water Resour. Res. 30, 2261–2285.
Katz, O., Reches, Z., Roegiers, J.-C., 2000. Evaluation of mechanical rock properties using a Schmidt Hammer. Int. J. Rock Mech. Min. Sci. 37, 723–728.
Lamb, M.P., Dietrich, W.E., 2009. The persistence of waterfalls in fractured rock. Geol. Soc. Am. Bull. 121 (7–8), 1123–1134.
Lamb, M.P., Fonstad, M.A., 2010. Rapid formation of a modern bedrock canyon by a single flood event. Nat. Geosci. 3 (7), 477–481.
Lamb, M.P., Howard, A.D., Dietrich, W.E., Perron, J.T., 2007. Formation of amphitheater-headed valleys by waterfall erosion after large-scale slumping on Hawai'i. Geol. Soc. Am. Bull. 119 (7–8), 805–822.
Lamb, M.P., Dietrich, W.E., Aciego, S.M., DePaolo, D.J., Manga, M., 2008. Formation of Box Canyon, Idaho, by megaflood: implications for seepage erosion on Earth and Mars. Science 320, 1067–1070.
Lamb, M.P., Finnegan, N.J., Scheingross, J.S., Sklar, L.S., 2015. New insights into the mechanics of fluvial bedrock erosion through flume experiments and theory. Geomorphology 244, 33–55.
Levin, H.L., 1989. Contemporary Physical Geology, 3rd ed. Saunders College Publ, Philadelphia.
Li, K.-W., Pan, Y.-W., Liao, J.-J., 2016. A comprehensive mechanics-based model to describe bedrock river erosion by plucking in a jointed rock mass. Environ. Earth Sci. 75, 517, 17 p. https://doi.org/10.1007/s12665-015-5113-0.
Mandych, A.F., 1935. Drought, Wind and Flood All Cause Soil Erosion. The Science News-Letter 28.747: 77. 2 May 2015. http://www.eolss.net/sample-chapters/c01/e4-06-02-06.pdf>.
McGinnis, R.N., Ferrill, D.A., Smart, K.J., Morris, A.P., Higuera-Diaz, C., Prawika, D., 2015. Pitfalls of using entrenched fracture relationships: Fractures in bedded carbonates of the Hidden Valley Fault Zone, Canyon Lake Gorge, Comal County, Texas. Am. Assoc. Pet. Geol. Bull. 99, 2221–2245.
McGinnis, R.N., Ferrill, D.A., Morris, A.P., Smart, K.J., Lehrmann, D., 2017. Mechanical stratigraphic controls on natural fracture spacing and penetration. J. Struct. Geol. 95, 160–170.
Moosdorf, N., Cohen, S., von Hagke, C., 2018. A global erodibility index to represent sediment production potential of different rock types. Appl. Geogr. 101, 36–44.
Morris, A.P., Ferrill, D.A., McGinnis, R.N., 2009. Mechanical stratigraphy and faulting in cretaceous carbonates. Am. Assoc. Pet. Geol. Bull. 93, 1459–1470.
Nield, M.C., 2018. Grout curtain construction at Bolivar Dam, Ohio. Environ. Eng. Geosci. 24 (1), 121–136.
Pan, Y.-W., Li, K.-W., Liao, J.-J., 2014. Mechanics and response of a surface rock block subjected to pressure fluctuations: a plucking model and its application. Eng. Geol. 171, 1–10.
Paola, C., Straub, K., Mohrig, D., Reinhardt, L., 2009. The "unreasonable effectiveness" of stratigraphic and geomorphic experiments. Earth Sci. Rev. 97, 1–43.
Scheingross, J.S., Lamb, M.P., 2017. A mechanistic model of waterfall plunge pool erosion into bedrock. J. Geophys. Res. Earth Surf. 122, 2079–2104. https://doi.org/10.1002/2017JF004195.
Stein, O.R., LaTray, D.A., 2002. Experiments and modeling of head cut migration in stratified soils. Water Resour. Res. 38 (12), 1284. https://doi.org/10.1029/2001WR001166.
Tinkler, K., 1987. Niagara Falls 1750-1845: the idea of a history and the history of an idea. Geomorphology 1, 69–85.
Tinkler, K.J., Pengelly, J.W., Parkins, W.G., Asselin, G., 1994. Postglacial recession of Niagara Falls in relation to the Great Lakes. Quat. Res. 42, 20–29.
Ward, W.C., Ward, W.B., 2007. Stratigraphy of the middle part of Glen Rose Formation (Lower Albian), Canyon Lake Gorge, central Texas. In: Scott, R.W. (Ed.), Cretaceous Rudists and Carbonate Platforms: Environmental Feedback, 87. SEPM Special Publication, pp. 193–210.
Webb, W.E., Hull, A.M., 1962. Engineering Geology of Canyon Dam, Guadalupe River, Comal County, Texas. Field Excursion #12: November 11, 1962. Geological Society of America Field Trip Guidebook, pp. 385–394.